Received: 8 April 2018 | Revised: 3 June 2019 | Accepted: 21 July 2019

DOI: 10.1002/pc.25360

RESEARCH ARTICLE

spe INSPIRING PLASTICS PROFESSIONALS Polymer COMPOSITES WILEY

Improvement of water vapor barrier and mechanical properties of sago starch-kaolinite nanocomposites

Jareerat Ruamcharoen[1] | **Ruszana Munlee**[1] | **Polphat Ruamcharoen**[2]

[1]Department of Science, Faculty of Science and Technology, Prince of Songkla University, Muang, Pattani, Thailand

[2]Rubber and Polymer Technology Program, Faculty of Science and Technology, Songkhla Rajabhat University, Muang, Songkhla, Thailand

Correspondence
Department of Science, Faculty of Science and Technology, Prince of Songkla University, Muang, Pattani 94000, Thailand.
Email: jareerat.su@psu.ac.th

Funding information
Prince of Songkla University, Pattani Campus Fund, Grant/Award Number: 59002

Abstract

The composite films of sago starch were prepared by incorporation of various amount of kaolinite (K) and kaolinite intercalated by dimethyl sulfoxide (DMSO) (KD) via solution blending method in order to reduce the water vapor transmission and enhance mechanical properties of starch based films. The kaolinite intercalation by DMSO and the composite films were characterized by using X-ray diffraction, Fourier transform infrared spectroscopy, and scanning electron microscope techniques. The result showed that well-dispersed kaolinite layers were delaminated in the starch matrix attesting to intercalate and exfoliate composite films. The effect of kaolinite content on the water vapor transmission and tensile properties of the composite films was investigated. The water vapor transmission of the starch film (neat starch film ca. 0.132 g. cm^3/h) decreased with the addition of K and KD to the starch. It was also observed that the maximum tensile strength (5.18 MPa) was attained for the composite film with 4% by weight of clay content. The improvement in the tensile strength and modulus of starch-based composites was due to the strong interfacial interaction between matrix and kaolinite clay, correlating to the change of morphology of the starch composite films as revealed by scanning electron microscopy.

KEYWORDS

biopolymers, films, nanocomposites, X-ray

1 | INTRODUCTION

Currently, the environmental pollution problem from consumed polymers has become serious, particularly from synthetic polymer materials. The biopolymer, which is environmental friendly, and biodegradable, is an ideal approach to solve this problem caused by synthetic polymer wastes.[1–4] Many types of starches are known to be completely biodegradable materials in soil and water, natural availability and renewability. As a result, it is one of the best candidates for replacing current synthetic polymers especially for packaging materials.[5–8] Recently, there have been many reports on cassava, potato, and corn starches based biopolymer films for packaging applications.[5–8] However, the starch is its pronounced water sensitive, the fast degradation rate and, in some cases, undesirable physical and mechanical properties.[3,7,9] Some procedures have been developed to enhance the barrier and mechanical properties of starch based composite films. The main procedures are the incorporation of new plasticizers such as urea/ethanolamine[9,10] and the use of clays to improve mechanical and barrier properties.[2,3,7,11–17] Clay is a potential filler; itself a naturally abundant mineral that is toxin-free and can be used as one of the components for food, medical, cosmetic, and healthcare recipients.[18–20] It should be highlighted that the work of starch-clay nanocomposites with mostly montmorillonite had been reported, while kaolinite-starch nanocomposites were not intensively studied.[21–24] This is due to the starch-kaolinite interactions are very weak as interlayer space of kaolinite is asymmetrical structure, permitting only particular reactions. The asymmetrical

structure of $AlO_2(OH)_4$ octahedral and SiO_4 tetrahedral sheets leads to induce strong superposed polarity, in conjunction with hydrogen bonds between the silicon oxide and the aluminol surface. As a result, the strong cohesive energy of the kaolinite mineral was found.[25] One of the solving methods is the preparation of the intercalated structure of kaolinite in starch composites, which are continually a great challenge. There are a few reports considering with kaolinite intercalation such as dimethyl sulfoxide (DMSO), poly(ethylene oxide), poly-3-hydroxybutyrate, and so on.[25,26] As already discussed, the starch-based nanocomposites have high potential applications in the packaging. There are important safety concerning about nanocomposite applications to food contact materials. Avella et al.[6] reported that migration of metals from the biodegradable starch/clay nanocomposite films used for packaging of vegetable samples was minimal. These materials can be applied for the food-packaging sector owing to their low overall migration limit. However, from the review of recent advances and migration issues in biodegradable polymers from renewable sources for food packaging by Scarfato et al.[27] and nano-food packaging, an overview of market, migration research, and safety regulations by Bumbudsanpharoke and Ko,[28] more studies are still needed to be re-investigated to demonstrate the conclusive statement.

Many studies have been reported on starch-based films made from various starches such as corn, potato, and cassava starch but very few works have been done on sago starch film.[29–31] Starch from sago palm (*Metroxylon sagu Rottb.*) is exclusively important socioeconomic crop in Southeast Asia. It has enormous potential to be explored to develop renewable biodegradable materials. Its granule typically contains ~26% to 31% amylose and 69% to 74% amylopectin. This is fulfilled the requirement of film forming capacity.[31] As sago starch has relatively high amylose content; as a result, better mechanical properties than those of other starches are obtained. However, as mentioned above, a moisture, water uptake, and water vapor permeability limit its potential to be employed as a basic raw material for developing biodegradable packaging.

The aim of this work is to prepare sago starch composite films in order to decrease water vapor transmission including with an improving mechanical properties of final product. The intercalated kaolinite was expected to play an important role for enhancing the physico-mechanical properties of starch based composite films.

2 | MATERIALS AND METHODS

2.1 | Materials

Sago starch was directly extracted from sago palm plant containing 24% of amylose (Amperometric titration with potassium iodate solution modified from McCleary et al.[32]), and 0.19% of protein content. The kaolinite clay was obtained from Amarin Clay Factory, (Thailand). The particle size of kaolinite was in the range of 2 to 10 μm. It was cleaned by immersing in concentrated HCl solution overnight to remove iron oxide. After washing, white clay was collected by filtration and dried in an oven at 60°C. Glycerol used as a plasticizer in starch film was purchased from Merck KGaA, Darmstadt (Germany). DMSO was purchased from BDH Laboratory Supplies (UK).

2.2 | Kaolinite-dimethylsulfoxide intercalation

The modification of kaolinite by dimethylsulfoxide (DMSO) was firstly performed by dispersion of kaolinite (10 g) into 100 mL distilled water, mixed with 90 mL of DMSO and then stirred at 80°C to form a suspension. After 24 h, the resulting material (kaolinite-DMSO) was washed several times with distilled water and then filtered. The wet kaolinite-DMSO was dried in a vacuum oven at 50°C to eliminate the DMSO adsorbing on the surface of the kaolinite.

2.3 | Preparation of starch-kaolinite composite films

The sago starch/kaolinite composite films were prepared by a solution-casting method. Three grams of starch were dispersed in distilled water and added glycerol (30 wt% of starch) at room temperature. The starch suspension was heated to the gelatinized temperature (80 ± 2°C) and continuously stirred. Subsequently, the clay suspensions varied from 2, 4, 6, and 8 wt% of starch were added to the gelatinized starch solution under stirring. The starch solution was cast onto polyethylene sheet mold and then dried at 50°C in an oven, and thickness of composite films with 0.25 ± 0.02 mm was obtained. The starch/kaolinite and starch/DMSO intercalated kaolinite were defined as SSK and SSKD, respectively.

2.4 | Characterization of starch based composite films

2.4.1 | X-ray diffraction technique

X-ray diffraction is an important method to quantify the intercalated/exfoliated structure of kaolinite in the composite films. X-ray diffraction was performed using a X-ray diffractometer X'Pert MPD, (PHILIPS, the Netherlands) with CuK_α radiation (λ = 0.154 nm) in operating at 40 kV and 30 mA. The diffraction patterns were recorded from 2.5 ° to 40° at a scanning rate 1°/min. The basal spacing of the silicate layer, d, was calculated using the Bragg's equation, $\lambda = 2d \sin\Theta$ (where Θ is the diffraction position and λ is the wavelength).

2.4.2 | Fourier transform infrared spectroscopy

The Fourier transform infrared (FT-IR) spectra of intercalated kaolinite and composite films were recorded in attenuated reflection mode using a spectrometer (Bruker, Billerica, Massachusetts) with a resolution of 4 cm^{-1}. The scanning of FT-IR spectra was in the wavenumber range of 4000 to 400 cm^{-1} with scan 32 times.

2.4.3 | Scanning electron microscopy

Scanning electron microscopy (SEM) was performed on a SEM-Quanta backscatter secondary electron detector (USA) for morphological study on the kaolinite, DMSO intercalated kaolinite and the starch composite films. The composite film was rapidly cooled in liquid nitrogen, and then fractured. The fractured samples were sputter-coated with gold before observation by SEM.

2.4.4 | Water vapor transmission test

Water vapor transmission of composite films was measured by cup method explained in ASTM E96-00 modified by Gontard et al.[33] A container with silica gel was closed with composite films firmly fixed on top. The container was placed in a desiccator which contained saturated sodium chloride solution, and condition was 75% relative humidity at 25°C. The film was weighed daily on an analytical balance until a constant weight was reached. At least three specimens for water vapor transmission tests were performed on each sample. The water vapor transmission (WVT) of composite films was calculated according to:

$$WVT\ \text{rate} = \frac{WG/t}{A}$$

Where WG is the weight gain, t is the time interval tested, and A is the sample area, respectively.

2.4.5 | Water absorption test

Prior to measurements, the composite films were oven dried at 60°C to constant weight. Afterward, each composite film was immersed in distilled water at 25°C for period of interval time. The composite film was removed from the distilled water and weight to obtain the final weight of swollen composite films. Water absorption test for each composite film was carried out in three replicates. The percentage of the water absorption of the composite films was calculated using the following equation:

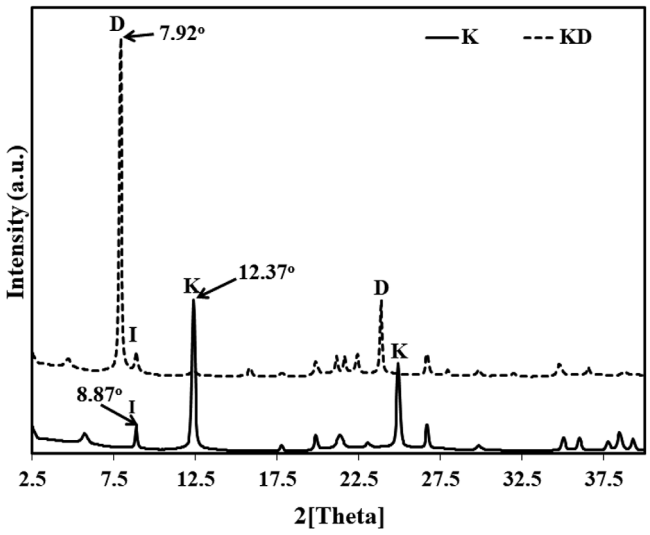

FIGURE 1 X-ray diffraction (XRD) patterns of kaolinite (K) and DMSO intercalated kaolinite (KD)

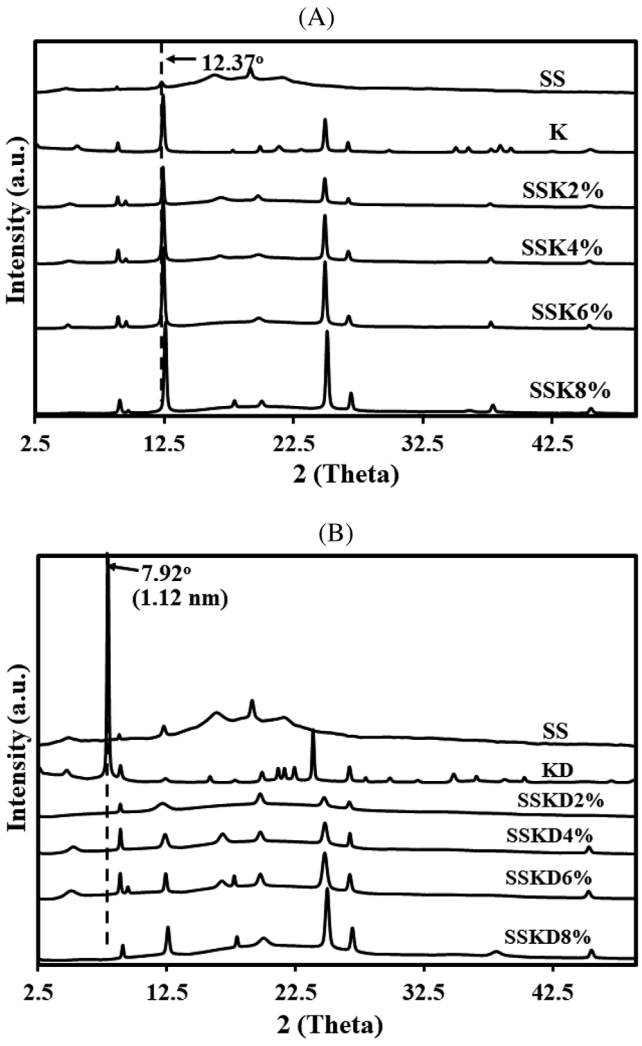

FIGURE 2 X-ray diffraction (XRD) patterns of composite films: SSK (A) and SSKD (B)

$$\text{Water absorption}\,(\%) = \frac{W_a - W_o}{W_o} \times 100$$

Where W_a is the weight of composite film at the water absorption, and W_o is the initial dry weight of the composite film.

2.4.6 | Tensile test

Tensile test was investigated using Hounsfield universal testing machine (UK) according to ASTM D 882-02. Specimen was cut into 120 × 12 mm in dimension, and conditioned at 50 ± 5% relative humidity, 25°C for 24 h. The crosshead speed was 50 mm/min. At least five specimens of each sample were tested and the average values of tensile strength, modulus, and elongation at break were reported.

3 | RESULTS AND DISCUSSION

3.1 | XRD data of clays and composite films

The XRD spectra of kaolinite (K) and kaolinite modified with dimethylsulfoxide (KD) are illustrated in Figure 1. The characteristic maximum of raw kaolinite was observed at 12.37° (very intense), corresponding to the basal spacing of kaolinite (0.72 nm). After DMSO intercalation, the XRD pattern of the kaolinite was changed. This agrees with previous reports.[21,22,25] The peak (2θ) at 12.37° in the kaolinite, shifted to small reflection angle at 7.92° resulting from a monolayer intercalation of the DMSO in the interlayer space.[22,25] This related to the shift of 0.72 nm basal spacing of the starting kaolinite upon intercalation of DMSO molecules to 1.12 nm. Inversely, the illite phase was not intercalated by DMSO molecules as proven by the characteristic peak (2θ) at 8.87° that remained unchanged.

Figure 2 shows the X ray diffraction spectra of composite films. The more intensity of peak at 12.37° was seen when increasing kaolinite content in the composite films as shown in Figure 2A. However, DMSO intercalated kaolinite was more disordered when incorporated in the SS matrix, as illustrated by the significantly decreasing intensity of peak at 7.92° (Figure 2B). This was indicated that the DMSO-intercalated kaolinite gave more dispersion in the starch matrix than unmodified kaolinite. Peak intensity at 7.92° was expected to increase. However, it was completely disappeared. This would be explained by two possibilities: (a) the complete exfoliation of kaolinite within the composite films and this result can be supported by morphology from SEM micrographs as shown in Figure 9. A similar observation was reported by Mbey et al. and (b) partially re-ordering to crystal form of KD. This relates to the appearing of small peaks at 12.37° for SSKD with 4, 6, and 8% of clay. As shown in Figure 2A,B, starch displayed the crystalline structure with diffraction peaks (2θ) at 12.89°, 17.27°, 19.83°, and 22.47°, respectively.[14,29] While there are less starch molecular crystal peaks observed for all composite films in Figure 2B, reflecting an amorphous structure of starch. This can be explained that intermolecular and intramolecular hydrogen bonds of starch chains were destructed in the starch gelatinization processing.[14,34,35]

3.2 | FT-IR analysis

The kaolinite, DMSO intercalated kaolinite, and composite films were characterized by FTIR spectroscopy. The presence of interlayer DMSO in kaolinite was revealed on the FT-IR spectrum (Figure 3) by the S—O stretching at 1095 cm^{-1} and by the modification of the external surface OH stretching mode at 3688, 3660, and 3628 cm^{-1} due to

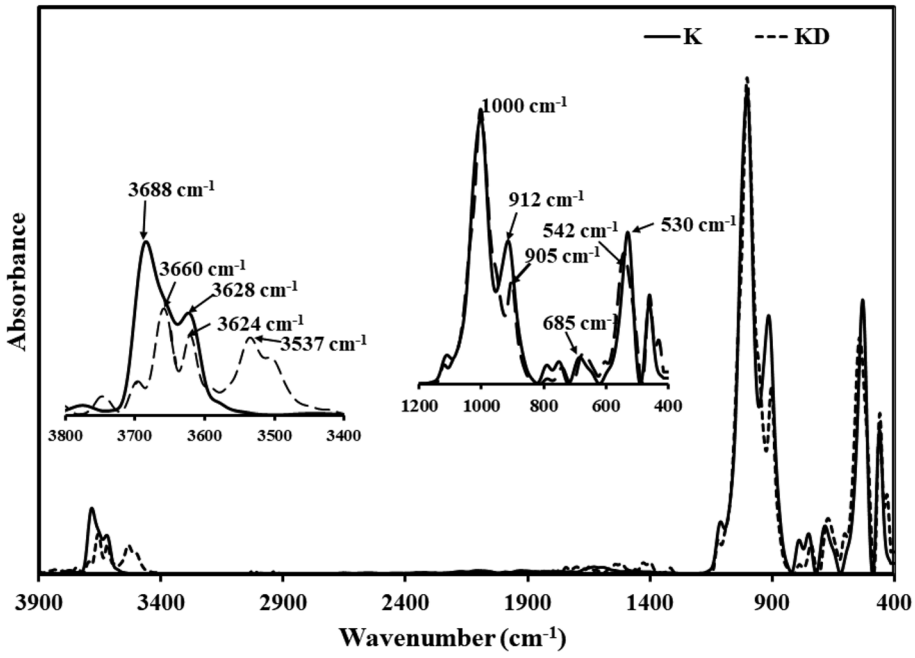

FIGURE 3 FT-IR spectra of kaolinite (K) and kaolinite intercalated with dimethyl sulfoxide (DMSO) (KD)

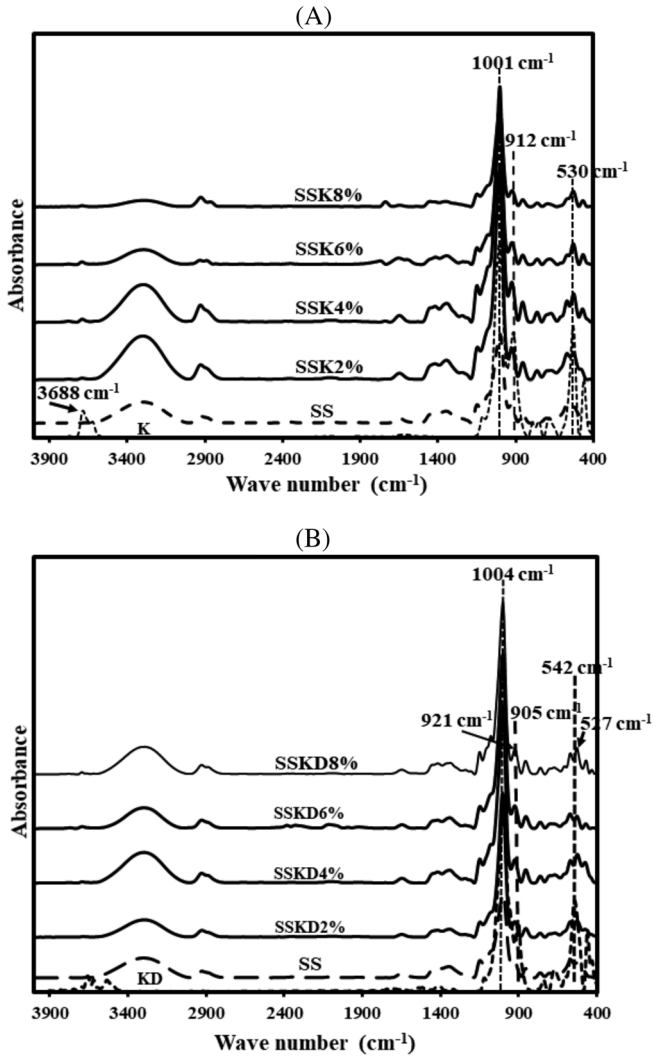

FIGURE 4 FT-IR spectra of composite films: SSK (A) and SSKD (B)

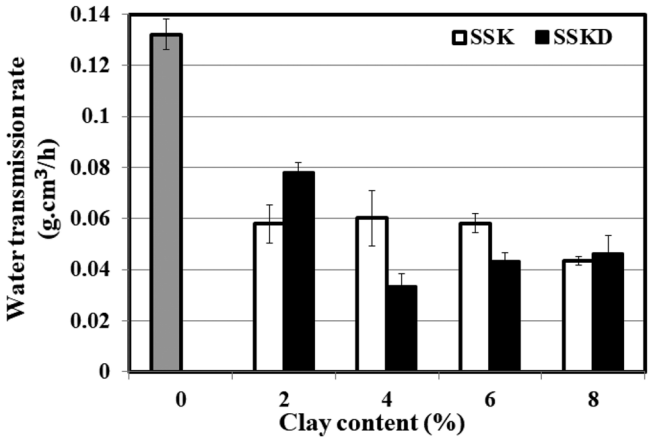

FIGURE 5 Water vapor transmission (WVT) of SSK and SSKD composite films

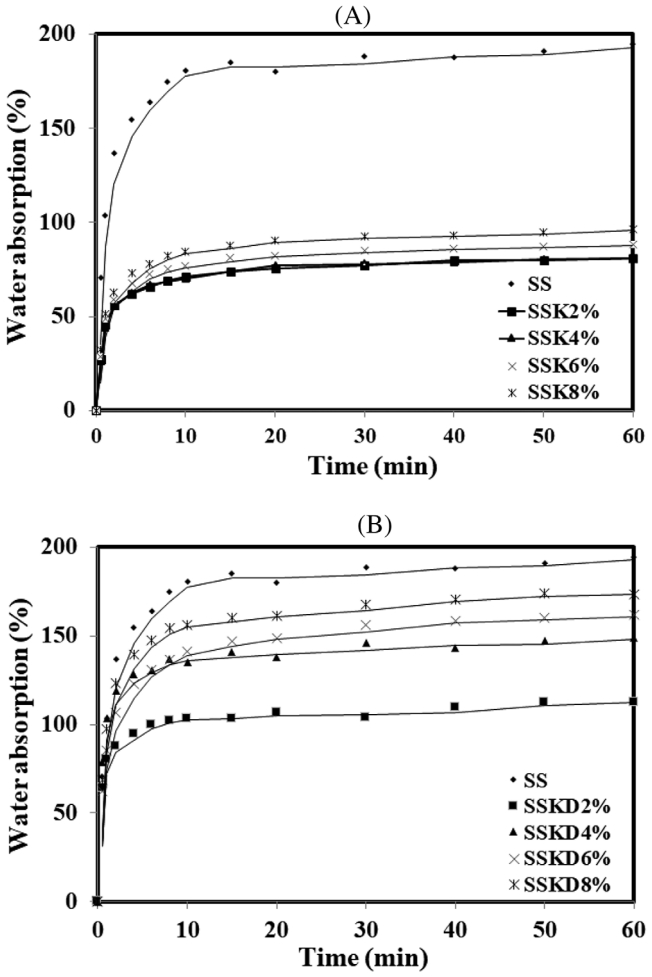

FIGURE 6 Water absorption of composite films: SSK (A) and SSKD (B)

interactions of the sulfonyl group in DMSO with the surface Al—OH groups of the clay. The peaks at 3537 and 3510 cm^{-1} accounted for the interaction of hydrogen of methyl group of the DMSO molecule with some hydroxyl groups of the kaolinite layer.[25] The peak at 912 cm^{-1} representing to O—H deformation linked to $2Al^{3+}$ mode shifted to higher wavelength, while the peak at 530 cm^{-1} assigning to Si—O—Al stretching mode of kaolinite shifted to lower wavelength due to interaction with DMSO.[25,36]

Interesting information of molecular structure can be derived from the FT-IR analysis. Difference between the FTIR spectra of SSK and SSKD composite films is shown in Figure 4.

In the presence of the unmodified kaolinite as a filler, the external surface O—H stretching at 3688 cm^{-1} of kaolinite and the bending mode of C—O—H bond of the starch at 995 cm^{-1} (Figure 4A) remain unchanged. This could be implied that some hydroxyl groups presenting on unmodified kaolinite clay had an interaction with glucopyranosyl units of starch chain by hydrogen bonding.[13] In addition, the shift of peaks at 997 and 542 cm^{-1} attributing to the antisymmetric and symmetric stretching vibrations of C—O—H bond of starch and Si—O bending of modified clay was observed. The Si—O—Al stretching of modified kaolinite at 542 cm^{-1} shifted to 527 cm^{-1}, due to the reduction of H-bonding of

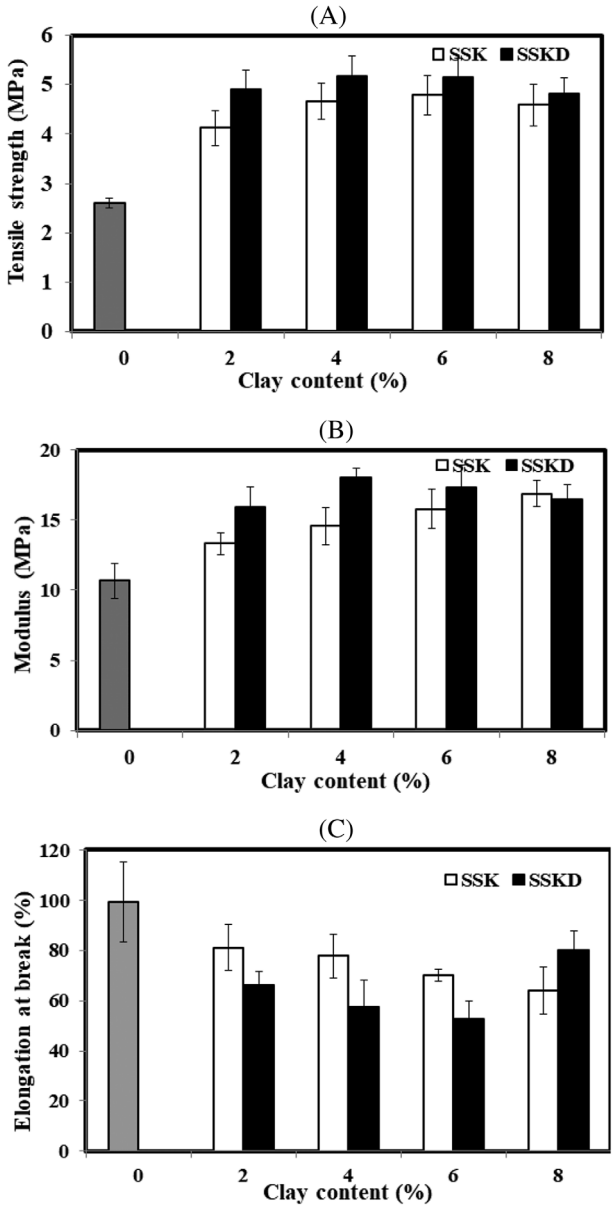

FIGURE 7 Tensile properties of the starch film and composite films: Tensile strength (A), modulus (B), and elongation at break (C)

between Si—O on the surface of kaolinite clay and hydrogen of methyl groups of DMSO intercalated kaolinite. It can be implied that the intercalation and exfoliation of modified clay present in the composite films. These results were consistent with those reported previously[7,37] indicating that the intercalation and exfoliation of modified clay were observed.

3.3 | WVT test and water absorption test

WVT is an important criterion to evaluate application of starch-based composite films. The WVT of the sago starch and the composite films with different clay contents are graphically shown in Figure 5. The WVT of the composite films decreased with incorporation of the kaolinite clay in the composite films. It can be clearly seen that the presence of kaolinite intercalated by DMSO significantly decreased the WVT of the composite films especially within 4 wt% of intercalated kaolinite (0.0335 g.cm^3/h). Compared to the neat sago starch film, the composite film with 4% wt of KD clay showed about a 75% decrease in WVT rate, while the composite film with 4% wt of kaolinite clay showed only 50% decrease. In gelatinization process of starch, the glycerol acted as a plasticizer, which entrapped between adjacent starch chains and decreased intermolecular attractions amount of starch chains, resulting in increasing molecular mobility. By this reason, the water vapor molecules can easily penetrate or diffuse into starch matrix.[16] Additionally, the decrease in the WVT of composite films caused by the incorporation of clay has also been observed by other researchers who work with starch and clay composites.[14,16,38] This can be explained that the modified clay causes the tortuous path for water vapor diffusion rising from exfoliation of clay.[14,16,35]

The water absorption of the starch and its composite films with different clay content is compared in Figure 6. The neat starch film showed the highest value for water absorption (ca. 200%) indicating that it had higher affinity for water than the composite films. This is due to the hydrophilic character of starch.[14,17,35] Nevertheless, the water absorption of composite films with unmodified kaolinite clay decreased, as shown in Figure 6A. It is most probably due to the H-bonding part of the water with the hydroxyl groups of the unmodified clay resulting in the decrease in water absorption of starch.[38,39]

However, it should be noted that the water absorption of SSKD films was obviously higher than SSK films and the water absorption increased with SSKD contents (Figure 6B). This could be explained that the partially re-ordering caused the agglomerate of clay. This result was supported by the larger agglomerate of clay and weak starch-clay interface (as seen in Figure 9E,F, respectively. The weak interface might cause more water penetration into the composite films.

3.4 | Tensile properties

The tensile strength, modulus, and elongation at break of SS and SS nanocomposites with different clay contents are illustrated in Figure 7. The addition of unmodified kaolinite and kaolinite intercalated with DMSO to starch films contributed to increase the tensile strength until the maximum value at 4%wt of kaolinite intercalated with DMSO, demonstrating that the starch chains were intercalated into the alumina-silicate layers. This behavior was expected and attributed to the stretching exerted by clay itself and to the orientation and aspect ratio of the intercalated silicate layers.[7,14,24] The oriented backbone of the polymer chains in the gallery bonded by hydrogen interaction enhanced the modulus and the stress. This result might have been observed because kaolinite had smaller sizes but more numerous particles dispersed in the starch, which could pose more restrictions to the movements

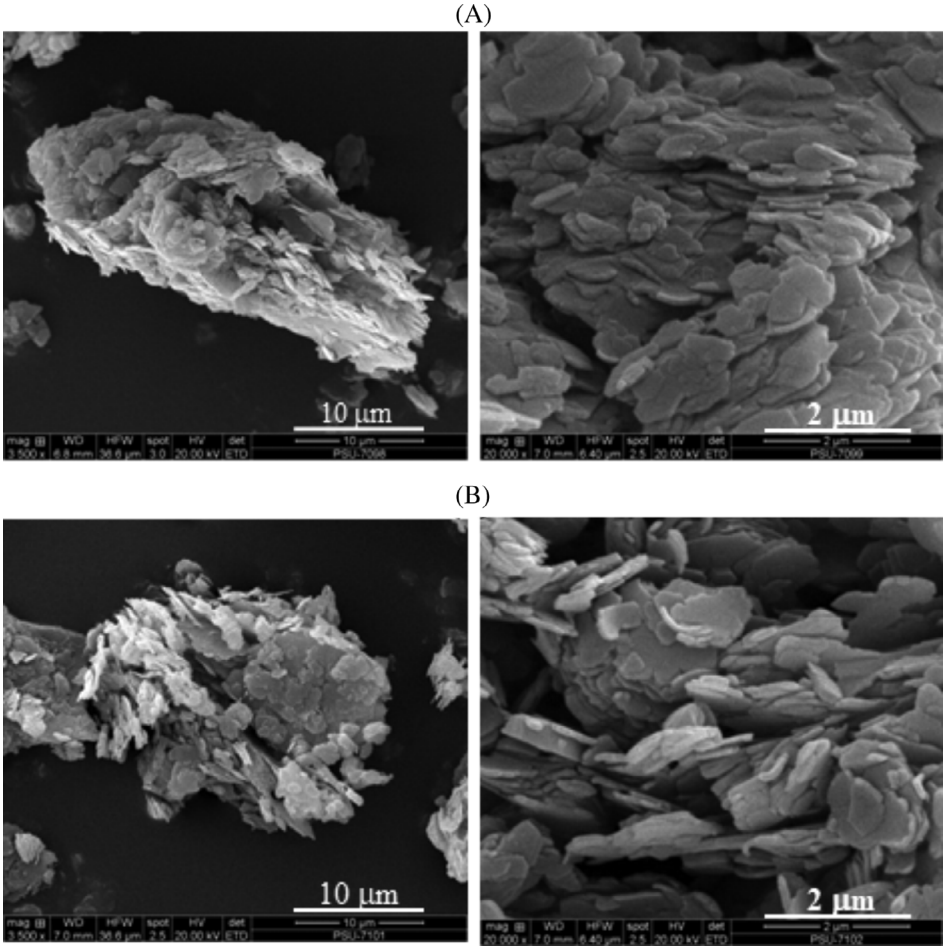

FIGURE 8 Scanning electron microscopy (SEM) micrographs of K (A) and KD (B) with magnification of ×1000 and ×20 000

of starch chains. According to Figure 7A,B, the tensile strength increased until it reached maximum value at 4 wt% of clay content and tended to constant. This could be explained that addition of more amount of clay into the matrix led to appearance of stacks and even aggregated clay.[3,5] The improvement was usually continued with increasing the clay content up to a percent at which the silicate layers could not be exfoliated anymore. Considering in Figure 7C, the decrease in elongation at break was observed when the kaolinite content increased. It could be explained that the addition of inorganic fillers to the starch increased its brittleness, as reported by other research groups.[7,17] The composites also displayed a noteworthy improvement in the mechanical properties particularly in the Young's modulus. The main reason for this improvement in the mechanical properties was the strong interfacial interaction between the matrix and layered silicate due to reduced starch chain mobility as the macroscopic rigidity of the film was enhanced.

3.5 | SEM morphology

The surface morphologies of kaolinite (K) and intercalated kaolinite (KD) were observed by SEM. As shown in Figure 8, the kaolinite appeared massive, as most lamellae were stacked together. After the kaolinite was modified with DMSO, the silicate layers took place and the interlayer distance of kaolinite clay increase. The lamellae were curled up and loosely packed, which confirms the intercalation of kaolinite lamellae by DMSO. As can be seen, kaolinite is composed of highly perfect small platelets, showing morphology with well define hexagonal edges.[26] SEM micrographs of the fracture surface were obtained for the starch and composites. The fracture surface of the starch film in Figure 9A exhibited the rather smooth surface. From SEM micrographs as shown in Figure 9B,C, the composite films containing 4 and 8%wt of clay revealed very coarse phase morphology. The white spots on the SEM micrographs represented particle size and distribution of silicate layer stacks in the matrix. This was due to the poor dispersion of clay platelets in composites. Then the platelets formed aggregates, which break upon loading as observed in the fracture surface of the starch composite films. It was an important to note that the starch-kaolinite clay interaction is very weak in the absence of a clay modification leading to inferior mechanical properties. Figures 9D,E clearly clarified that 4 and 8%wt of kaolinite intercalated DMSO influenced the morphology. It was apparent that clay particles were uniformly dispersed in the starch matrix. As the clay content increased to 8 wt%, some form aggregates of platelets were observed (Figure 9(E)). It was reported by Cyras et al., that in the intercalated composites the clay platelets were poorly dispersed

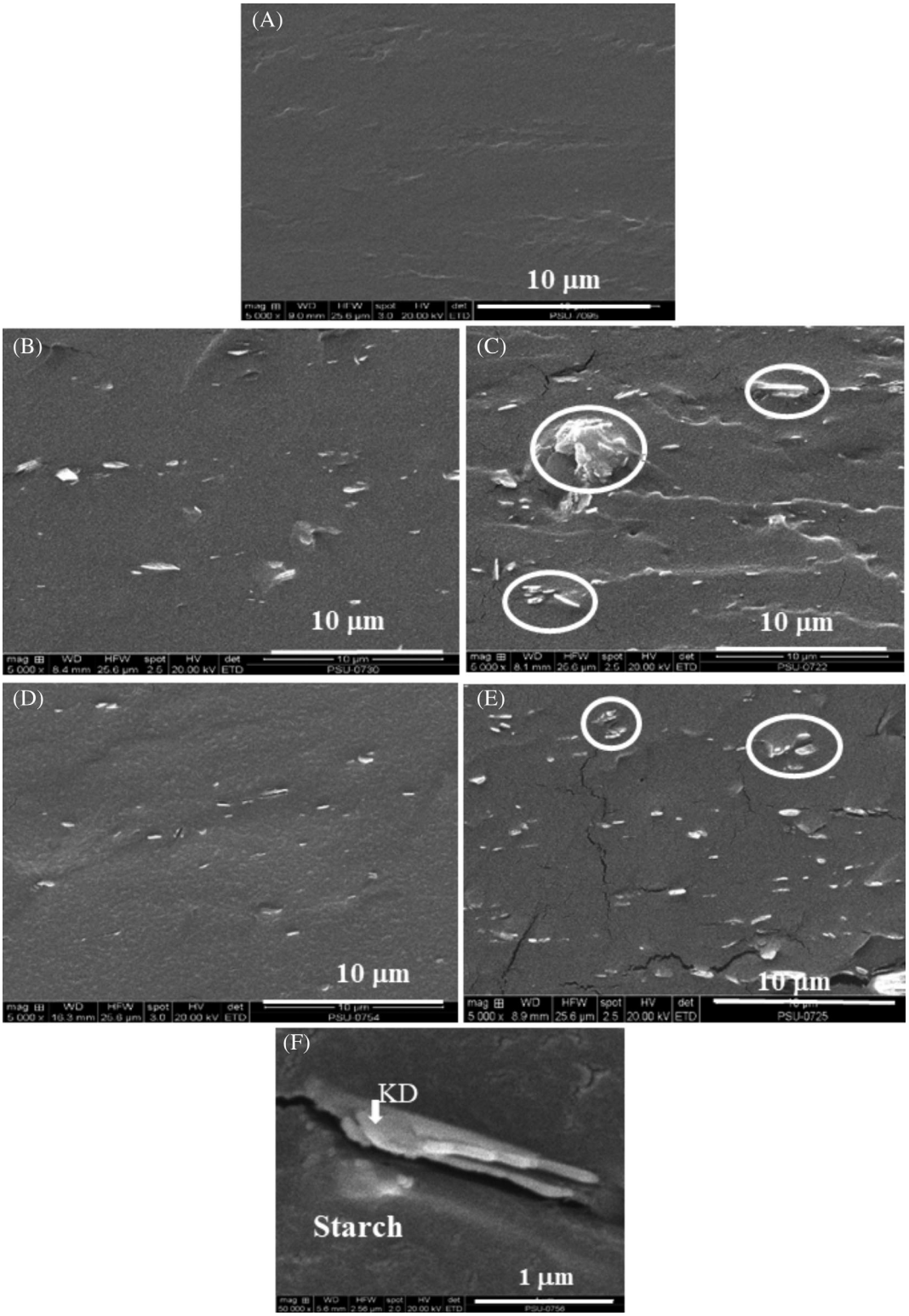

FIGURE 9 Scanning electron microscopy (SEM) micrographs of fracture surface of composite films: sago starch (A), SSK4% (B), SSK8% (C), SSKD4% (D), SSKD8% (E) with 5 kX, and (F), SSKD4% with 50 kX

and that form aggregates break upon loading. The evidence of the SEM micrographs corresponded to the tensile behaviors of composite films as shown in Figure 7. The silicate layers were expanded and gave nanosize dispersion in the starch matrix, hence they played an important role in reinforcing action into the matrix as illustrated in Figure 9F. Increasing the clay content nevertheless conducted to an agglomerate formation, as demonstrated for 8 wt% clay, resulting in the reduction of physico-mechanical properties of the composite films. A similar observation was obtained in other reports.[3,7,17]

4 | CONCLUSIONS

An improvement of WVT and absorption including with tensile properties of sago starch film was achieved by kaolinite and modified kaolinite. The use of DMSO intercalated kaolinite was advantageous for the clay dispersion and distribution, which enhance the effect of clay content on starch film properties. An increment in the interlayer distance of the kaolinite clay in the composite films was observed by X-ray diffraction providing evidence that the nanolayer silicates formed an intercalated structure without reach a complete exfoliation. The decrease in WVT rate was observed for the composite films because of the degree of dispersion of the clay pellets within the starch matrix. The composite films presented a remarkable improvement in the mechanical properties such as Young's modulus and tensile strength. However, a diminution in the deformation was observed due to the reinforcing action of kaolinite intercalated by DMSO. The main reason for this development in the properties in starch-based composites was the strong interfacial interaction between starch matrix and clay and then changed the morphology of the matrix of starch. Nevertheless, further research is necessary to improve their mechanical and barrier properties for a packaging film to withstand external stress and maintain its integrity as well as barrier properties during applications in food packaging.

ORCID

Jareerat Ruamcharoen https://orcid.org/0000-0003-2979-0651

REFERENCES

[1] Q. X. Zhang, Z. Z. Yu, X. L. Xie, K. Naito, Y. Kagawa, *Polymer* **2007**, *48*, 7193.
[2] V. P. Cyras, L. B. Manfredi, M. T. Ton-That, A. Vázquez, *Carbohydrate Polymers* **2008**, *73*, 55.
[3] F. A. Aouada, L. H. C. Mattoso, E. Longo, *Indus. Crops Products* **2011**, *34*, 1502.
[4] H. M. Park, W. K. Lee, C. Y. Park, W. J. Cho, C. S. Ha, *J. Mater. Sci.* **2003**, *38*, 909.
[5] S. Mali, L. S. Sakanaka, F. Yamashita, M. V. E. Grossmann, *Carbohydrate Polymers* **2005**, *60*, 283.
[6] M. Avella, J. J. de Vlieger, M. E. Errico, S. Fischer, P. Vacca, M. G. Volpe, *Food Chem.* **2005**, *93*, 467.
[7] K. Majdzadeh-Ardakani, A. H. Navarchian, F. Sadeghi, *Carbohydrate Polymers* **2010**, *79*, 547.
[8] J. W. Rhim, H. M. Park, C. S. Ha, *Prog. Polymer Sci.* **2013**, *38*, 1629.
[9] C. Zeppa, F. Gouanve, E. Espuche, *J. Appl. Polymer Sci.* **2009**, *112*, 2044.
[10] F. Xie, E. Pollet, P. J. Halley, L. Averous, *Prog. Polymer Sci.* **2013**, *38*, 1590.
[11] B. Chen, J. R. G. Evans, *Carbohydrate Polymers* **2005**, *61*, 457.
[12] D. Schlemmer, R. Angelica, M. J. A. Sales, *Comp. Struct.* **2010**, *92*, 2066.
[13] H. Liu, D. Chaudhary, S. I. Yusa, M. O. Tade, *Carbohydrate Polymers* **2011**, *83*, 1591.
[14] C. M. O. Müller, J. B. Laurindo, F. Yamashita, *Indus. Crops Products* **2011**, *33*, 605.
[15] C. M. O. Müller, J. B. Laurindo, F. Yamashita, *Carbohydrate Polymers* **2012**, *89*, 504.
[16] A. C. Souza, R. Benze, E. S. Ferrão, C. Ditchfield b, A. C. V. Coelho, C. C. Tadini, *LWT - Food Science Technol.* **2012**, *46*, 110.
[17] P. Müller, E. Kapin, E. Fekete, *Carbohydrate Polymers* **2014**, *113*, 569.
[18] E. H. Bakraji, J. Karajou, *J. Trace Microprobe Tech.* **2003**, *21* (2), 397.
[19] K. B. P. N. Jinadasa, C. B. Dissanayake, *Environ. Geochem. Health* **1992**, *14*(1), 3.
[20] J. T. Pang, C. H. Fan, X. J. Liu, T. Chen, G. X. Li, *Biosensors Bioelectron.* **2003**, *19*(5), 441.
[21] X. Zhao, B. Wang, J. Li, *J. Appl. Polymer Sci.* **2008**, *108*, 2833.
[22] J. A. Mbey, S. Hoppe, F. Thomas, *Carbohydrate Polymers* **2012**, *88*, 213.
[23] P. Lu, M. Zhang, P. Qian, Q. Zhu, *Polymer Composites* **2012**, *33*, 889.
[24] J. A. Mbey, F. Thomas, *Carbohydrate Polymers* **2015**, *117*, 739.
[25] J. A. Mbey, F. Thomas, S. Ngally, C. J. Liboum, D. Njopwouo, *Appl. Clay Sci.* **2013**, *83-84*, 327.
[26] J. E. Gardolinski, L. C. M. Carrera, *J. Materials Sci.* **2000**, *35*, 3113.
[27] P. Scarfato, L. D. Maio, L. Incarnato, *J. Appl. Polymer Sci.* **2015**, *132*, 1. https://doi.org/10.1002/app.42597.
[28] N. Bumbudsanpharoke, S. Ko, *J. Food Sci.* **2015**, *80*, 910.
[29] F. B. Ahmad, P. A. Williams, J.-L. Doublier, S. Durand, A. Buleon, *Carbohydrate Polymers* **1999**, *38*, 361.
[30] H. Ismail, N. F. Zaaba, *J. Vinyl Additive Technol.* **2012**, *18*, 235.
[31] C. D. Poeloengasih, F. D. Anggraeni, *Starch* **2014**, *66*, 1103.
[32] B. V. McCleary, T. S. Gibson, M. D. C. Mugford, *J. AOAC* **1997**, *80*, 571.
[33] N. Gontard, S. Guilbert, J. L. Cuq, *J. Food Sci.* **1993**, *58*, 206.
[34] S. Rahman, *Food Properties Handbook*, 2nd ed., CRC, Boca Raton, FL, USA **1995**.
[35] S. Wang, C. Li, L. Copeland, Q. Niu, S. Wang, *Comp. Rev. Food Sci. Food Saf.* **2015**, *14*, 568.
[36] B. J. Saikia, G. Parthasarathy, *J. Modern Phys.* **2010**, *1*, 206.
[37] L. S. Loo, K. K. Gleason, *Macromolecules* **2003**, *36*, 2587.
[38] G. Harikrishnan, T. U. Patro, D. V. Khakhar, *Ind. Eng. Chem. Res.* **2006**, *45*, 7126.
[39] M. K. S. Monteiro, V. R. L. Oliveira, F. K. G. Santos, E. L. Barros Neto, R. H. L. Leite, E. M. M. Aroucha, R. R. Silva, K. N. O. Silva, *Food Res. Int.* **2018**, *105*, 637.

How to cite this article: Ruamcharoen J, Munlee R, Ruamcharoen P. Improvement of water vapor barrier and mechanical properties of sago starch-kaolinite nanocomposites. *Polymer Composites*. 2020;41: 201–209. https://doi.org/10.1002/pc.25360